

Laser microengineering of photonic devices in glass

Kazuyoshi ITOH*

* *Department of Material and Life Science, Graduate School of Engineering, Osaka University, 2-1 Yamadaoka, Suita, Osaka 565-0871, Japan*
E-mail: itoh@mls.eng.osaka-u.ac.jp

We have been studying the refractive index changes and vacancies that are induced in transparent materials like glass by the irradiation of femtosecond laser pulses. This technique has been applied to fabricate three-dimensional photonic structures such as optical data storages, waveguides, gratings, and couplers inside a wide variety of transparent materials. We report micro-fabrication experiments of optical elements in glasses with femtosecond laser pulses, including fabrication of couplers, Bragg gratings, and zone plates and holograms on the surface of glass. A trial fabrication experiment on organic materials is also reported.

Keywords: femtosecond, laser pulse, fabrication, three-dimensional, optical elements

1. INTRODUCTION

Micromachining by femtosecond laser pulses in transparent materials has recently received much attention. When femtosecond laser pulses are focused inside the bulk of a transparent material, the intensity in the focal volume can become high enough to cause nonlinear absorption, which leads to localized modification in the focal volume, while leaving the surface unaffected. Recent demonstrations of three-dimensional micromachining of glass using femtosecond laser pulses include waveguides [1-9], couplers [10-14], gratings [15-23], and three-dimensional binary data storage [24-27], lenses [28,29], and channels [30-33]. We present, in this paper, fabrication experiments of three-dimensional photonic devices. Contents of this paper are based on those presented in the International Symposium on Advances and Trends in Fiber Optics and Applications (ATFO 2004), October 11-15, 2004, Chongqing University, Chongqing, China, and The 6th International Symposium on Laser Precision Microfabrication – SCIENCE AND APPLICATIONS – (LPM2005), April 4-8, Williamsburg, Virginia, USA. A 2-mm-long directional coupler to split the optical beam intensities into 1:1 at a wavelength of 632.8 nm is demonstrated [14]. We present in this paper the fabrication experiment of volume gratings induced in silica glass by filamentation of ultrashort laser pulses [17]. We stacked the layers with a period of several microns and fabricated volume gratings. To measure the diffraction efficiency we entered a He-Ne laser beam at the wavelength of 632.8 nm to the grating with the Bragg angle. The maximum diffraction efficiency was 74.8% with the grating that had the period of 3 μm , and the thickness of 150 μm . Fresnel zone plates by embedding voids in silica glass are demonstrated [28]. Holographic data storage on fused silica, soda-lime, and lead glasses with a single 130 fs laser pulse at a wavelength of 800 nm is presented [22]. After the sample is exposed to the interference fringe pattern of the object beam and the reference beam, a relief hologram is recorded through surface ablation. The recorded information can be reconstructed without destruction of the hologram when the power of the reference beam is reduced below the ablation threshold. Finally, we show

the formation of three-dimensional channels with microscopic diameters by in-water ablation of silica glass [33].

2. WAVEGUIDE AND COUPLER

Direct writing of optical devices using femtosecond laser pulses in glass has potential applications in the telecommunication industry. The induction of permanent refractive-index change at the laser focal point has been reported in the bulk of glasses to the order of 10^{-2} to 10^{-4} [1]. By translation of the sample with respect to the focal point, fabrication of waveguides [1-9] and couplers [10-14] has been demonstrated. Techniques for fabricating waveguides can be divided into two categories: side writing and parallel writing. In side writing, the sample is translated perpendicularly to the laser beam. This method can fabricate long waveguides, but the symmetry of the core of the waveguide is broken by the intensity distribution. When the laser pulses are focused by a high-NA objective to reduce asymmetry of the intensity distribution, the three-dimensional volume of the sample cannot be fully accessed because of the short working distance of the objective. In parallel writing, laser pulses are focused into the sample by a low-NA lens having a long working distance, and the sample is translated parallel to the propagation axis of the laser pulses. The length of the waveguide is then restricted by the working distance of the focusing objective. However, parallel writing can fabricate waveguides having symmetrical cores and can make full use of the three-dimensional volume. The quality of the waveguide may be degraded by the laser pulses being affected by spherical aberration at different depths. In both methods, to create high-quality waveguides, the total fluence at a single spot needs to be controlled, and this depends on the pulse energy and scanning speed. Attempts to fabricate waveguides having high index changes by translation of the sample at low speed or by exposure to higher energies lead to waveguide damage, with void-like damages having been observed as the result of optical breakdown.

We have reported that filamentation of femtosecond laser pulses induces permanent refractive-index change in silica glass [3]. Filamentation occurs due to a balance be-

tween the Kerr self-focusing of the laser pulse and the defocusing effect of the high-intensity plasma generated in the self-focal region. Experiments in this paper were performed using a regeneratively amplified Ti:Sapphire laser system which produces 130 fs, 800 nm, 1 kHz pulses. The laser pulses propagate along the optical axis (+z direction). The sample was a piece of SiO₂ glass. The sample was mounted on a computer-controlled three-axis motion stage, and was illuminated by a halogen lamp from one side perpendicularly to the optical axis of the ultrashort pulses and observed from the other side using an objective lens and a charge-coupled device (CCD) camera. The region of refractive index change was 10 to 500 micrometers long due to the NA of the focusing lens used on the silica glass. Although the plasma density induced in the filament is not high enough to produce optical breakdown, the plasma absorbs pulse energy nonlinear ionization can induce refractive index changes. By translation of the sample parallel to the optical axis, the 2-mm straight waveguides was fabricated. In this section, we report three-dimensional couplers by filamentation of femtosecond laser pulses [14].

We fabricated directional couplers containing a 2-mm-long straight waveguide and a curved waveguide connected to a different straight section. Laser pulses were focused into the sample by a 0.30-NA objective lens. Laser pulse energy was adjusted to 0.68 $\mu\text{J}/\text{pulse}$ by neutral density filters to form a single filament. The length of the filament was 40 μm . The straight section was parallel to the straight waveguide and was separated by a 4- μm center-to-center distance, which was the minimum separation in the experiment. The straight waveguide was fabricated using a translation speed of 0.2 $\mu\text{m}/\text{s}$. Another straight waveguide was then fabricated parallel to the straight waveguide. The curved waveguide was fabricated from one end of the straight section by scanning the sample in the x - z direction. The position of the filament was determined by computer-controlled positioning along an arc of radius 17 mm. For radii greater than 17 mm, smooth curved waveguides could be obtained. Several couplers were fabricated by varying the length of the straight sector L .

Coupling properties were investigated by focusing a He-Ne laser beam having a wavelength of 632.8 nm into the straight. Experimental results that the splitting ratios of the directional couplers with $L = 1$ mm and $L = 0.5$ mm are approximately 1:1 and 1:0.5, respectively. Experimental results show that splitting ratio depends on interaction length L , and that this behavior is a typical characteristic of directional couplers.

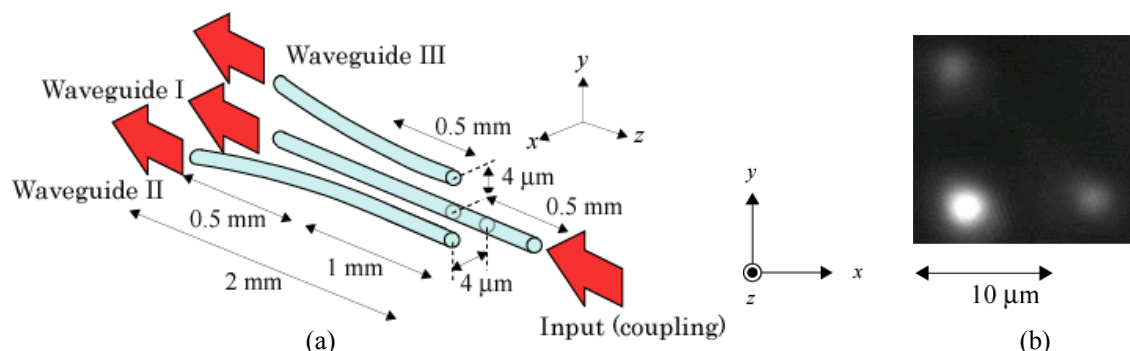


Fig. 1 Schematic of a three-dimensional directional coupler. Near-field patterns of coupler output when coupling to a He-Ne laser at a wavelength of 632.8 nm.

Producing real three-dimensional photonic devices is one of the salient features of femtosecond micromachining. We demonstrate the realization of three-dimensional directional couplers using filamentation. Figure 1 (a) shows the schema of a three-dimensional directional coupler consisting of three waveguides: a 2-mm-long straight waveguide (waveguide I) and two curved waveguides that are connected to straight sections (waveguide II and III). The curved waveguides have arc radii of 17 mm. The straight sections of waveguide II and III were parallel to the straight waveguide at a 4 μm center-to-center separation in the x and y directions, respectively. Lengths of the straight sectors in waveguide II and waveguide III were 0.5 mm and 1.0 mm. The He-Ne laser beam was first coupled to the straight waveguide and the NFPs (Near-field patterns) were monitored using a black and white CCD camera. Figure 1 (b) shows the NFPs of beams from the coupler at a wavelength of 632.8 nm. The beam was split amongst the three waveguides at different intensities.

3. VOLUME GRATING

The volume grating with a fine period is an important device because of its large diffraction angle, high diffraction efficiency, and high wavelength selectivity. There are two methods of fabricating the grating with femtosecond laser pulses inside silica glass. One is the two-beam interference method [19-23]. The grating is created by two-beam interference of a split single pulse. The grating usually has a fine period of less than 1 μm and can be recorded only by a single pulse. However the diffraction efficiency of the grating is very low (1 %) and it is difficult to control its thickness and three-dimensional shape. The other is the direct-writing method [15,16]. The fabrication time is longer, however, one can vary the thickness and period of the grating. We report fabrication of Bragg grating by scanning the filament two-dimensionally perpendicular to the optical axis inside the silica glass [17].

The laser pulses with energy of 1.0 μJ were focused in silica glass with a 0.10 NA focusing lens. A 150- μm -long filament was formed. When the filament was scanned for 300 μm along the x -axis (perpendicular to optical axis) at the speed of 1 $\mu\text{m}/\text{s}$, a layer of refractive-index change with a thickness of 2 μm was induced. The laser pulses were linearly polarized. We stacked 60 layers along the y -axis with a sample displacement of 5 μm . Figure 2 shows optical images of the fabricated gratings. Figure 2 (a) shows the top view of the grating that was observed from the z -axis. Figures 2 (b) and 2 (c) are the side views that are ob-

served from the x - and the y -axes, respectively.

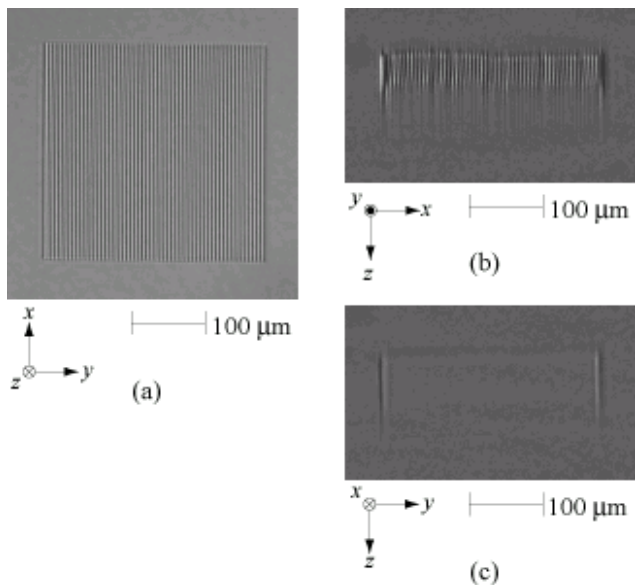


Fig. 2 Optical images of the fabricated gratings with the period of $5\ \mu\text{m}$ and thickness of $150\ \mu\text{m}$. The fabrication energy was $1.0\ \mu\text{J}$ and the translation speed of the filament was $1\ \mu\text{m/s}$. (a) Top view. (b) Side view (xz -plane). (c) Side view (yz -plane).



Fig. 3 Schematic of diffraction pattern. The fabricated grating with the period of $3\ \mu\text{m}$ and thickness of $150\ \mu\text{m}$. The fabrication energy was $1.0\ \mu\text{J}$ and translation speed of the filament was $1\ \mu\text{m/s}$.

To investigate the characteristics of the gratings, we fabricated several different gratings by varying the thickness and period. To change the thickness of gratings, we chose three different lenses, namely, the 0.05, 0.10, and 0.30 NA lenses. The translation speed of the filament was fixed to $1\ \mu\text{m/s}$. The size of the gratings was $300\ \mu\text{m} \times 300\ \mu\text{m}$ in the xy -plane. The diffraction efficiency of the grating was measured with a cw He-Ne laser at the wavelength of $632.8\ \text{nm}$. The angle of the He-Ne beam with respect to the grating vector was adjusted to achieve the maximum diffraction efficiency. The maximum diffraction efficiency of 74.8 % was obtained with TE polarization (electric field perpendicular to the plane of incidence) of the reading beam when the grating was fabricated using the 0.10 NA focusing lens and with a period of $3\ \mu\text{m}$. The profile and image of the diffraction pattern are shown in Fig. 3. When the period of the grating pattern was narrowed, the diffraction efficiency was increased. The angles between the transmitted zeroth-order beam and the first-order diffraction beams were ~ 7.5 , 9.3 , and 12.2 degrees in the cases of the periods of 5 , 4 , and $3\ \mu\text{m}$, respectively. The angles agreed with Bragg's law.

4. FRESNEL LENS

Tightly focusing femtosecond laser pulses with high NA lenses produce submicron-damage inside a wide variety of transparent [24-27]. The damage appears as cavities or voids with diameters of only $200\ \text{nm}$ to $1\ \mu\text{m}$, surrounded by densified material. We are presenting in this section the report of fabrication of a lens by embedding voids inside silica glass [28].

Figure 4 (a) shows the schematic of the designed Fresnel lens. Fresnel zone plate consists of a series of disks centered at one point with a radius of s_1 , $s_1 + 1/2$, $s_1 + 1$, $s_1 + 3/2$, and so forth, where s_1 is the radius of the first odd zone and l is the wavelength. When we block either all the even or all the odd zones, this zone plate has a focusing property. In our layout, light passes through only the odd zones in the zone plate, and light cannot transmit in the

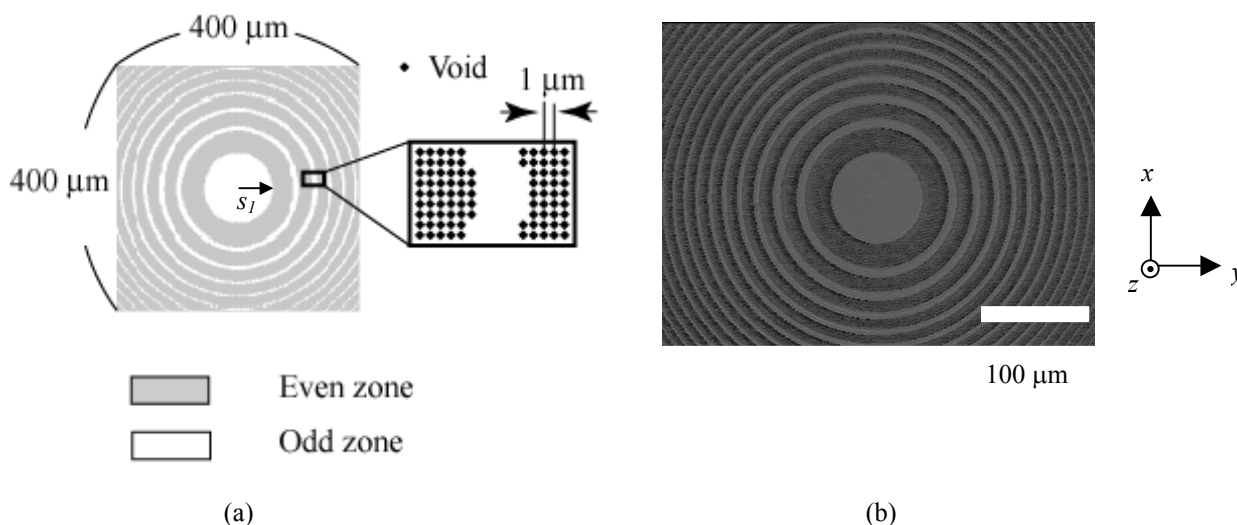


Fig. 4 (a) Schematic of the fabrication of Fresnel zone plate. We constructed the zone plate that passes only the odd zones and obstructs the even zones. Even zones are fabricated by embedding the array of the voids with steps of $1\ \mu\text{m}$. (b) Optical image of the fabricated Fresnel zone plate by embedding the two-dimensional array of voids.

even zones. Even zones are fabricated by embedding the array of the voids to block light. Our designed Fresnel lens has the primary focal length of 3 mm at the wavelength of 632.8 nm. The radius of the first odd zone was designed to be 43.5 μm . The size of the zone plate was 400 $\mu\text{m} \times 400 \mu\text{m}$. In this condition, the radius of the outer zone is 200 μm , which corresponds to the included number of the odd zone plate is eleven.

The laser pulses were tightly focused by an objective lens with a NA of 0.55 to create the voids inside silica glass, which was 3 mm thick. We fabricated the Fresnel zone plate by embedding voids at the depth of 300 μm beneath the sample of silica glass. In the following experiment, we set the energy to be 0.4 μJ /pulse to produce one layer of the zone plate by embedding voids. The sample was displaced dot by dot in the xy -plane perpendicular to the laser propagation axis by steps of 1 μm with a computer-controlled motor stage. Figure 4 (b) shows an optical image of the fabricated Fresnel zone plate by embedding the two-dimensional array of voids. The image was observed under halogen lamp illumination. The voids were embedded only in the even zones.

We investigated the focusing properties of the fabricated Fresnel zone plate. The beam incident on the lens is diffracted and converges in on the primary focal spot on the optical axis. The He-Ne laser beam was launched into the zone plate and a diffracted beam was focused on the surface of a CCD camera. The measured spot size was 7.0 μm and agreed with the theoretical value of 6.1 μm . The measured diffraction efficiency was 2.0 %

5. HOLOGRAM

A holographic grating can be encoded on the surface or inside nonphotosensitive glasses by two beam interference of a single near infrared femtosecond laser pulse [19-23]. The diffraction efficiency of a surface relief grating can reach 20%. These experiments suggest the potential of holographic optical storage in nonphotosensitive glasses, however, no storage of actual data image has been realized until 2002 [22]. In this section, we present experimental results of holographic data storage on the surface of fused silica, soda-lime, and lead glasses by two-beam interference of a single 130 fs laser pulse at a wavelength of 800 nm [22].

A top view of the experimental schema for recording and reconstruction of a data image is shown in Fig. 5. A binary data mask consists of a two dimensional array of 9 spots arranged in 3-column by 3-row. The spot distance both in horizontal and vertical directions are ~ 3 mm. A laser pulse is split into the reference and object beams. The two beams are incident onto the sample at approximately equal angles. The angle between them is set to be 33° . The Fourier transform configuration is used to record the information. A hologram is written when the reference beam intersects with the object beam and their interference fringes are recorded in the sample. The data image can then be reconstructed by illumination of the hologram with the reference beam. By use of a second lens behind the sample to perform a second Fourier transformation, the data information can be retrieved by a CCD camera. When the optical paths are adjusted to give a perfect spatial and temporal overlap of the reference and object beams on the surface of

the sample, we can observe a clear fringe pattern with an optical microscope. The reference beam is reduced below the ablation threshold. Three samples were used in our experiments: fused silica, soda-lime glass, and lead glass. The energies of the reference beam and object beam are 130 μJ and 110 μJ per pulse, respectively. Under these energy, only part of the fringes whose intensities are above the ablation threshold are recorded in the hologram as shown in Fig. 6 (a). The replicated fringes in the hologram discontinue at places where the fluence are below the ablation threshold, resulting in dimmer spots at the four corners of the reconstructed image as shown in Fig. 6 (b). When the soda-lime glass with a lower threshold is used, more fringes can be recorded. Figure 6 (c) illustrates a hologram on a soda-lime glass plate under the same experimental

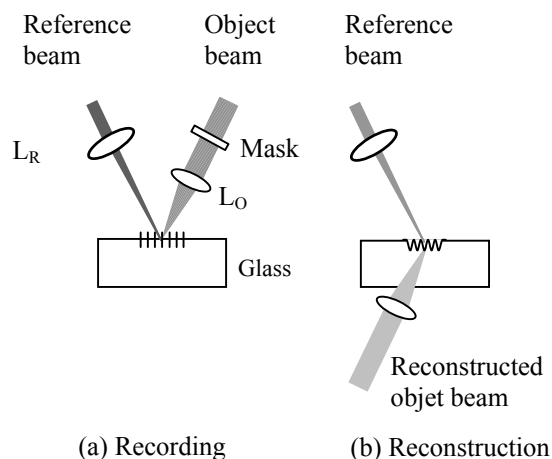


Fig. 5 Top view of experimental schematics for (a) hologram recording and (b) reconstruction of data.

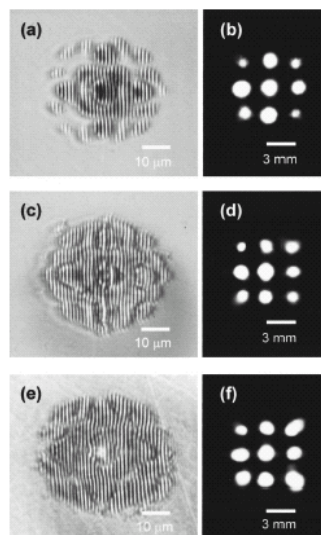


Fig. 6 Holograms recorded on fused silica, soda-lime, and lead glasses and their corresponding reconstructed images. (a) A hologram on fused silica glass and (b) the corresponding reconstruction data; (c) a hologram on soda-lime glass and (d) the corresponding reconstruction data; (e) a hologram on lead glass plate and (f) the corresponding reconstruction data.

conditions. The reconstructed image shown in Fig. 6 (d) is better than that in Fig. 6 (b) on fused silica. Soda-lime glass is the most common and the least expensive form of glass, therefore, this technique may open a frontier in holographic data storage. Because the lead glass has a much lower threshold, we can record a hologram with weaker energy. Figure 6 (e) shows a typical micro hologram on lead glass, which is recorded after the incident energy is reduced to one-third. The reconstructed data image is shown in Fig. 6 (f). All nine spots are clearly retrieved.

6. MICRO-CHANNEL

We embedded a diffraction grating in bulk PMMA (polymethylmethacrylate) by producing periodical structural changes. In order to produce the periodic structure, the sample was translated perpendicularly to the laser beam axis (x -axis) at a velocity of 5 mm/s. Each single pulse produced each 125- μm -long filamentary cavity with a period of 5 μm in the sample at the 1-kHz repetition rate of the laser pulses. Figure 7(a) shows a part of the fabricated periodical structure. When a He-Ne laser beam with a wavelength of 632.8 nm was incident normally on the fabricated periodic structure, a diffraction pattern with many orders was observed. Figure 7(b) shows the far-field diffraction pattern. The diffraction efficiency of the first order was approximately 2.9%. The filamentary structural change was revealed to be a cylindrical cavity based on the observation with a SEM (scanning electron microscope), observation of capillary action of water in the cavity, and analysis of diffraction by an embedded diffraction grating. When the pulse energy was 2.0 $\mu\text{J}/\text{pulse}$, the cavity had a diameter of 0.8 μm and a length of 125 μm . We measured the diameter and length by SEM observation.

7. MICRO-CHANNEL

I reviewed the topic of laser fabrication of photonic devices in silica glass focusing on our recent works. The fabrication of 2 mm directional couplers to split a beam into 1:1 at a wavelength of 632.8 nm was demonstrated. Realization of three-dimensional directional couplers was also demonstrated. We demonstrated the fabrication experiment of the volume gratings induced by the self-trapped long filament of the femtosecond laser pulses. The thickness of the grating was controlled by varying the filament length with the numerical apertures of the focusing lens. The

maximum diffraction efficiency of the fabricated grating was 74.8 %. We fabricated the Fresnel zone plate, which size was 400 $\mu\text{m} \times 400 \mu\text{m}$ by embedding voids in silica glass. The collimated He-Ne laser beam was launched into the zone plate and investigated the focusing properties. The spot size of the primary focal point was 7.0 μm and agreed well with the theoretical value of 6.1 μm . The diffraction efficiency was 2.0 %. This technique enables us to make alignment free micro-scale lenses inside bulk materials. We demonstrated the fabrication experiment of the volume gratings induced by the self-trapped long filament of the femtosecond laser pulses. Holographic data storage on the surface of fused silica, soda-lime, and lead glasses is presented. The relief microhologram is recorded through surface ablation on a nonphotosensitive glass plate after the sample is exposed to the interference fringe of object beam and reference beam that are split from a single femtosecond pulse. Fabrication of three-dimensional microchannels is potential use for μ -TAS application.

ACKNOWLEDGEMENTS

The experiments reported in this paper were conducted mostly at the Venture Business Laboratory, Osaka University.

References

- [1] K. M. Davis, K. Miura, N. Sugimoto, and K. Hirao, *Opt. Lett.* **21**, pp. 1729-1731, 1996.
- [2] K. Miura, J. Qiu, H. Inouye, T. Mitsuyu, and K. Hirao, *Appl. Phys. Lett.* **71**, pp. 3329-3331, 1997.
- [3] K. Yamada, T. Toma, W. Watanabe, J. Nishii, and K. Itoh, *Opt. Lett.* **26**, pp. 19-21, 2001.
- [4] C. B. Schaffer, A. Brodeur, J. F. Garca, and E. Mazur, *Opt. Lett.* **26**, pp. 93-95, 2001.
- [5] M. Will, S. Nolte, B. N. Chichkov, and A. Tunnermann, *Appl. Opt.* **41**, pp. 4360-4364, 2002.
- [6] S. Nolte, M. Will, J. Burghoff, and A. Tuennermann, *Appl. Phys A* **77**, pp. 109-111, 2003.
- [7] A. Saliminia, N. T. Nguyen, M. -C. Nadeau, S. Petit, S. L. Chin, and R. Vallée, *J. Appl. Phys.* **93**, pp. 3724-3728, 2003.
- [8] G. Cerullo, R. Osellame, S. Taccheo, M. Marangoni, D. Polli, R. Ramponi, P. Laporta and S. De Silvestri, *Opt. Lett.* **27**, 1938-1340, 2002.
- [9] Y. Tokuda, M. Saito, M. Takahashi, K. Yamada, W.

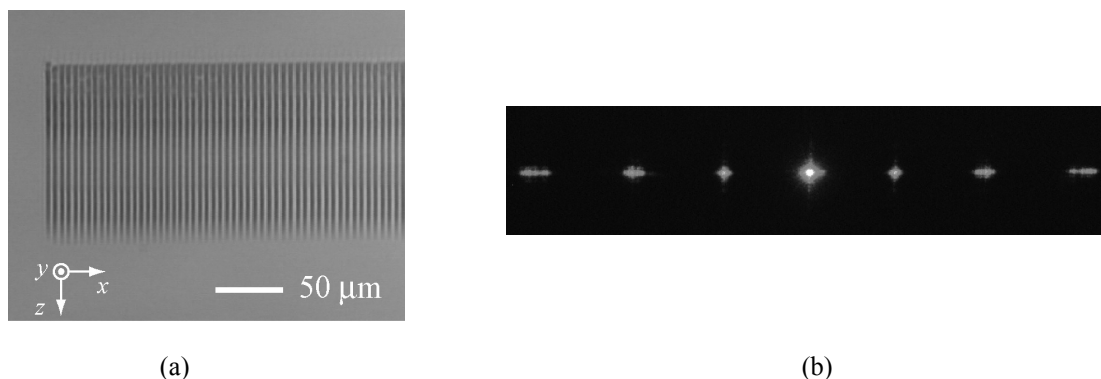


Fig. 7 Micrograph of a grating formed in PMMA (a) and its diffraction pattern (b).

- Watanabe, K. Itoh, and T. Yoko, *J. Non-Cryst. Solids* **326&327**, pp. 472-475 (2003).
- [10] D. Homoelle, W. Wielandy, A. L. Gaeta, E. F. Borrelli, and C. Smith, *Opt. Lett.* **24**, pp. 1311-1313, 1999.
- [11] A. M. Streltsov and N. F. Borrelli, *Opt. Lett.* **26**, pp. 42-44, 2001.
- [12] K. Minoshima, A. M. Kowalevicz, I. Hartl, E. P. Ippen, and J. G. Fujimoto, *Opt. Lett.* **26**, pp. 1516-1518, 2001.
- [13] K. Minoshima, A. M. Kowalevicz, E. P. Ippen, and J. G. Fujimoto, *Opt. Express* **10**, pp. 645-652, 2002.
- [14] W. Watanabe, T. Asano, K. Yamada, K. Itoh, and J. Nishii, *Opt. Lett.* **28**, pp. 2491-2493, 2003.
- [15] L. Sudrie, M. Franco, B. Prade, A. Mysyrowicz, *Opt. Commun.* **171**, pp. 279-284, 1999.
- [16] T. Toma, Y. Furuya, W. Watanabe, J. Nishii, K. Hayashi, and K. Itoh, *Opt. Rev.* **7**, pp. 14-17, 2000.
- [17] K. Yamada, W. Watanabe, K. Kintaka, J. Nishii, and K. Itoh, *Jpn. J. Appl. Phys.* **42**, pp. 6916-6919 (2003).
- [18] K. Yamada, W. Watanabe, J. Nishii, and K. Itoh, *J. Appl. Phys.* **93**, pp. 1889-1892 (2003).
- [19] Y. Li, W. Watanabe, K. Yamada, T. Shinagawa, and K. Itoh, J. Nishii, and Y. Jiang, *Appl. Phys. Lett.*, **80**, pp. 1508-1510, 2002.
- [20] K. Kawamura, T. Ogawa, N. Sarukura, M. Hirano, and H. Hosono, *Appl. Phys. B* **71**, pp. 119-121, 2000.
- [21] K. Kawamura, M. Hirano, T. Kamiya, and H. Hosono, *Appl. Phys. Lett.* **81**, pp. 1137-1139, 2002.
- [22] Y. Li, W. Watanabe, K. Itoh, and X. Sun, *Appl. Phys. Lett.* **81**, pp. 1952-1154, 2002.
- [23] Y. Li, K. Yamada, T. Ishizuka, W. Watanabe, K. Itoh, and Z. Zhou, *Opt. Express* **10**, pp. 1173-1178, 2002.
- [24] E. N. Glezer, M. Milosavljevic, L. Huang, R. J. Finlay, T.-H. Her, J. P. Callan, and E. Mazur, *Opt. Lett.* **21**, pp. 2023-2025, 1996.
- [25] E. N. Glezer and E. Mazur, *Appl. Phys. Lett.* **71**, pp. 882-884, 1997.
- [26] W. Watanabe, T. Toma, K. Yamada, J. Nishii, K. Hayashi, and K. Itoh, *Opt. Lett.* **25**, pp. 1669-1671, 2000.
- [27] W. Watanabe and K. Itoh, *Opt. Express* **10**, pp. 603-608, 2002.
- [28] W. Watanabe, D. Kuroda, K. Itoh, and J. Nishii, *Opt. Express* **10**, pp. 978-983, 2002.
- [29] E. Bricchi, J. D. Mills, P. G. Kazansky, B. G. Klappauf, and J. J. Baumberg, *Opt. Lett.* **27**, 2200-2202, 2002.
- [30] Y. Kondo, J. Qiu, T. Mitsuyu, K. Hirao, and T. Yoko, *Jpn. J. Appl. Phys.* **38**, pp. L1146-L1148, 1999.
- [31] A. Marcinkevicius, S. Juodkazis, M. Watanabe, M. Miwa, S. Matsuo, H. Misawa, and J. Nishii, *Opt. Lett.* **26**, pp. 277-279, 2001.
- [32] M. Masuda, K. Sugioka, Y. Cheng, N. Aoki, M. Kawachi, K. Shihoyama, K. Toyoda, A. Helvajian, and K. Midorikawa, *Appl. Phys. A* **76**, 857-860, 2003.
- [33] Y. Li, K. Itoh, W. Watanabe, K. Yamada, D. Kuroda, J. Nishii, and Y. Jiang, *Opt. Lett.* **26**, pp. 1912-1914, 2001.

(Received: April 4, 2005, Accepted: July 19, 2005)